Determination of Linear and Non-linear Hydrodynamic Derivatives of a Surface Ship in Manoeuvring Using CFD Method

Sheeja Janardhanan and Parameswaran Krishnankutty

Abstract Ensuring navigational safety of a vessel entails the determination of the manoeuvring coefficients or the hydrodynamic derivatives and the subsequent simulation of its trajectory well in advance of constructing the ship and this task is indeed a very challenging one. The number of hydrodynamic derivatives to be determined is based on the mathematical model used for the representation of hydrodynamic forces and moments. This chapter presents the mathematical formulation of the problem and the numerical approach used for obtaining the hydrodynamic derivatives. For this, an attempt has been made to numerically simulate the conventional horizontal planar motion mechanism (HPMM) towing tank experiment using the RANSE CFD model. A container ship model has been modelled for performing simulation andanalysis. The numerical tank size has been set following the ITTC guidelines, applying the grid size of 600,000 hexahedral cells. The free-surface effects have been taken into account. The prescribed body motions have been modelled by using the mesh morphing ANSYS CFX technique with 3-modes motion viz. pure sway, pure yaw and combined sway and yaw motions, referred as combined motions in this chapter. The time histories of forces and moments have been approximated with the Fourier series in order to enable the comparison with the corresponding equations for forces and moments, as represented by the developed mathematical model defined with linear and non-linear hydrodynamic derivatives. These computed derivatives have been compared with the experimental results, showing reasonably good agreement.

Keywords Ship manoeuvring · Hydrodynamic derivatives · Planar motion mechanism · CFD simulation

S. Janardhanan (✉) · P. Krishnankutty
Mechanical Engineering, SCMS School of Engineering and Technology, Karukutty, Ernakulam, India
e-mail: sheejajanardhanan@scmsgroup.org

D. Vucinic et al. (eds.), *Advances in Visualization and Optimization Techniques for Multidisciplinary Research*, Lecture Notes in Mechanical Engineering, https://doi.org/10.1007/978-981-13-9806-3_4

Nomenclature

a_{dMm}	Fourier constants associated with cosine terms
A	Derivatives evaluated and deemed very important
b_{dMm}	Fourier constants associated with sine terms
B	Beam of the vessel
C	Derivatives evaluated and deemed of minor importance
C_B	Block coefficient of the vessel
D	Derivatives evaluated and deemed negligible
D_t	Depth of the vessel
L	Length between perpendiculars of the vessel
m	Integer for determining harmonics of Fourier series
N	Hydrodynamic reaction moment in yaw
N_{HN}	Hydrodynamic reaction moment in yaw in pure yaw mode
N_{HY}	Hydrodynamic reaction moment in yaw in pure sway mode
N_{HYN}	Hydrodynamic reaction moment in yaw in combined motion
r	Yaw rate
r_a	Amplitude of yaw rate
r'_a	Non-dimensional amplitude of yaw rate
$\dot{y}'_{0a}$	Non-dimensional amplitude of yaw rate
t	Instantaneous time
T	Time period of oscillation
T_a	Draft at aft of the vessel
T_f	Draft at fore of the vessel
T_m	Mean draft of the vessel
u	Forward velocity in ship-fixed co-ordinate system
u_0	Forward velocity in early-fixed co-ordinate system
u^+	Non-dimensional velocity
u_{aN}	Amplitude of surge velocity in pure yaw mode
u_{aYN}	Amplitude of surge velocity in pure yaw mode
u_{cN}	Constant in surge velocity in pure yaw mode (Eq. 26)
u_{cYN}	Constant in surge velocity in combined motion (Eq. 44)
v	Sway velocity in ship-fixed co-ordinate system
v_0	Sway velocity in earth-fixed co-ordinate system
v_{aYN}	Amplitude of sway velocity in combined motion
V	Resultant velocity
x	Position in longitudinal direction in ship-fixed co-ordinate system
x_0	Position in longitudinal direction in earth-fixed co-ordinate system
X	Non-dimensional hydrodynamic reaction force in surge
X_{HN}	Hydrodynamic reaction force in surge in pure yaw mode
X_{HY}	Hydrodynamic reaction force in surge in pure sway mode
X_{HYN}	Hydrodynamic reaction force in surge in combined motion
y	Position in transverse direction in ship-fixed co-ordinate system
y^+	Non-dimensional wall distance
y_0	Position in transverse direction in earth-fixed co-ordinate system

y_{0a} Amplitude of sway motion
Y Non-dimensional hydrodynamic reaction force in sway
Y_{HN} Hydrodynamic reaction force in sway in pure yaw mode
Y_{HY} Hydrodynamic reaction force in sway in pure sway mode
Y_{HYN} Hydrodynamic reaction force in pure sway in combined motion

Greek Symbols

β Drift angle
β_a Drift angle amplitude
γ Arbitrary value of phase which depends on the start value of oscillation
∇ Volumetric displacement of the vessel
ω Circular frequency of oscillation
ω' Non-dimensional circular frequency of oscillation
ψ Heading/yaw angle
ψ_a Amplitude of yaw angular motion

1 Introduction

Manoeuvring or steering of ships is generally concerned about their motions produced as a result of excitation forces applied through the deflection of control surfaces in the absence of excitation from the sea (calm water). The motion of the surface ship can be described using the 2 dimensional reference frame. The fixed earth reference frame defines the inertial frame of reference, while the ship reference frame is fixed to the ship gravity centre and moves together with the ship. Figure 1 shows the definition of the ship co-ordinate systems. In a pure mathematical sense, the ship manoeuvrability depends on the hydrodynamic coefficients or derivatives, which are the acceleration coefficients, defined as the velocity terms in the manoeuvring equations of motion.

The most challenging part of the ship manoeuvring simulation is the estimation of these derivatives. These derivatives need to be estimated and the manoeuvrability of the ship must be assessed well in advance to meet the standards of safe navigation. Experimental, theoretical and numerical methods are used for the hydrodynamic derivatives estimation. The experimental methods employing captive model tests have been used for the calculation of hydrodynamic derivatives from the measured forces and moments. The free-running model tests have yet another experimental method, which is more straightforward for predicting the trajectory and controllability assessment, while the captive model tests are more versatile, as the stability indices and forces, contributing to the manoeuvring motion, can be quantified with these tests. The hydrodynamic derivatives, which are determined through the captive model tests, can also be used in designing the autopilot.

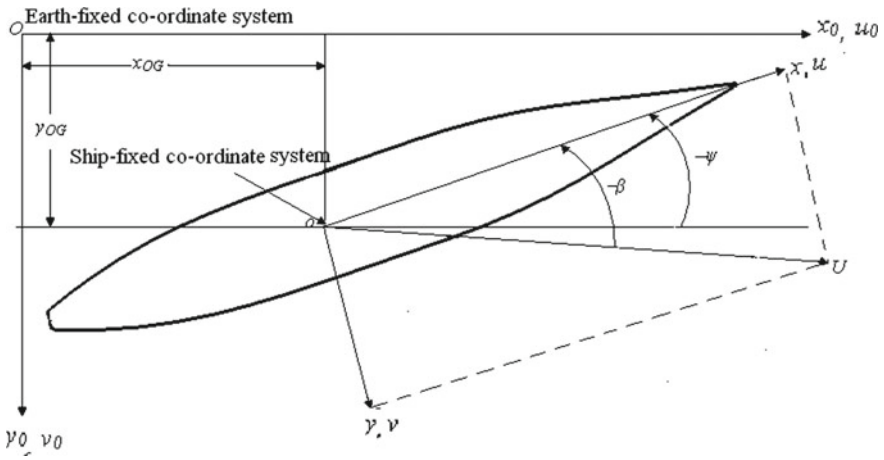

Fig. 1 Manoeuvring reference frames

The drawback of the experimental methods is the huge cost and involved experimental resources. The theoretical methods, based on a number of assumptions, on the other side have their own limitations as far as the accuracy is concerned. These difficulties have paved a glorious path in applying the numerical methods. The numerical methods are quite efficient in accomplishing simulations (duplicating experiments) and with related flow visualizations, they reduced the tedious model-testing task to become the computer modelling and simulation task. As indirectly mentioned with the "reducing" term, these techniques are not full-fledged, and will never replace the experiments, but will surely reduce their number to minimum. Nevertheless, they definitely seem to be very promising to be researched and developed in the years to come.

The past decade has brought with it, a host of numerical methods, which find easy implementation, with the tremendous advance in digital computing. Initially, numerical methods have been based on the potential flow theory, and have been used for the determination of the first order hydrodynamic derivatives. However, these methods have failed in predicting these derivatives successfully as they lacked adequate flow physics by not taking into account the viscous effects. With the emergence of the CFD based Reynolds Averaged Navier-Stokes Equations (RANSE), a powerful tool in flow prediction and associated phenomenon, the research focus has been set to explore its efficacies in the field of ship hydrodynamics, such as resistance and propulsion, sea keeping, manoeuvring etc. Especially, manoeuvring estimations demand attention, as safety issues in navigation have become prime concern as per IMO regulations. This factor has further strengthened the need for using CFD methods in this domain, and thus, brings to light the present research scenario in this field. For instance, Toxopeus [1] developed a mathematical model based on the bare hull forces and moments in steady drift, steady yaw and combined drift and yaw motions using the viscous flow

calculations. Carrica and Stern [2] used DES simulations to assess the manoeuvrability of a tanker, by bringing about 35-degree rudder turn and 20/20 zig-zag manoeuvre.

Janardhanan and Krishnankutty [3] determined the sway velocity dependency on the linear and non-linear hydrodynamic derivatives of a container ship, by simulating straight line tests using the RANSE equations for wider range of drift angles. Nonaka et al [4] estimated the hydrodynamic forces acting on the ship during manoeuvring motion using CFD. Sulficker [5] has explained the simulation of HPMM for the evaluation of linear derivatives, where the derivatives have been determined by using the forces and moments obtained at the maximum velocities and acceleration points, without creating an extensive formulation problem to carry out such simulations.

Cura-Hochbaum [6] determined the linear hydrodynamic derivatives of a passenger ship model by simulating the viscous flow around the hull, undergoing forced motions using a RANSE solver. The free-surface effects have not been considered in this work. This method was extended to the tanker models by simulating the combined sway and yaw by Cura-Hochbaum et al. [7]. The trajectories of the vessels were also simulated using the estimated derivatives. Xing-Kaeding and Jensen [8] presented the CFD modelling of the hull, rudder and propeller, together with the estimation of forces and moments during a turning circle and zig-zag manoeuvres. Tyagi and Sen [9] have shown the procedure for estimating the transverse velocity, applying the linear and non-linear AUV derivatives. Ohmori [10] numerically simulated the straight-line test, circular motion test and planar motion mechanism tests, to find the transverse force acting on the hull based on the velocity dependent linear derivatives. All these remarkable contributions indicate the important impact of the RANSE based CFD calculations to the manoeuvring analysis.

This book chapter focuses on the method development for determining the hydrodynamic derivatives in conjunction with a numerical horizontal planar motion mechanism test based on the CFD simulations. The performed RANSE simulations employ the finite volume technique for solving the viscous fluid flow equations. A container ship model (S175) [11] has been used for the presented analysis. Figure 2 shows the container ship model geometry, as generated by using the ANSYS ICEM CFD software package, and Table 1 shows the model particulars.

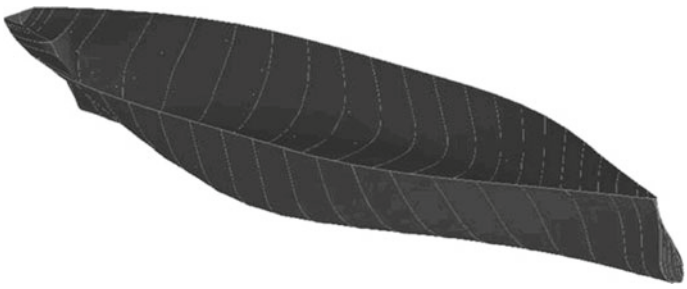

Fig. 2 Container ship model (up to LWL)

Table 1 Particulars of the container ship

Particular	Ship	Model (scale 1:36)
L (m)	175	4.86
B (m)	25.4	0.705
T_f (m)	8.0	0.22
T_a (m)	9.0	0.25
T_m (m)	8.5	0.236
D_t (m)	11	0.305
∇ (m^3)	21,222	0.4548
C_B	0.559	0.559

2 Mathematical Model

A mathematical model representing surface ship manoeuvring comprises the equations of motion in surge, sway and yaw modes, where the influence of other modes on manoeuvring are generally assumed as being insignificant. For ships, which take strong manoeuvres, the roll mode of the motion and its influence on the above-mentioned modes becomes considerable. A mathematical model is obtained by expanding the hydrodynamic reaction force or moment for each mode applying the Taylor series [12]. The retention of the higher order terms results in obtaining the non-linear models.

Any manoeuvring problem involving the estimation of hydrodynamic derivatives starts with the selection of an appropriate mathematical model. In this work the model proposed by Son and Nomoto [11] has been used after neglecting the roll effects where the speed and steering are given by simplifying Eqs. (1)–(3).

$$X = X(u) + (1-t)T + X_{vr}vr + X_{vv}v^2 + X_{rr}r^2 + X_{\delta}\sin\delta + X_{ext} \tag{1}$$

$$Y = Y_v v + Y_r r + Y_{vvv}v^3 + Y_{rrr}r^3 + Y_{vvr}v^2 r + Y_{vrr}vr^2 + Y_{\delta}\cos\delta + Y_{ext} \tag{2}$$

$$N = N_v v + N_r r + N_{vvv}v^3 + N_{rrr}r^3 + N_{vvr}v^2 r + N_{vrr}vr^2 + N_{\delta}\cos\delta + N_{ext} \tag{3}$$

The hydrodynamic terms can be separated out and the equations can be rearranged as:

$$\begin{aligned} X_H = {} & X_{\dot{u}}\dot{u} + Y_{\dot{v}}vr + X_{uu}u|u| + (1-t)T + X_{vr}vr \\ & + X_{vv}v^2 + X_{rr}r^2 + X_{\delta}\sin\ \delta \end{aligned} \tag{4}$$

$$\begin{aligned} Y_H = {} & X_{\dot{u}}ur + Y_{\dot{v}}\dot{v} + Y_{\dot{r}}\dot{r} + Y_v v + Y_r r + Y_{vvv}v^3 \\ & + Y_{rrr}r^3 + Y_{vvr}v^2 r + Y_{vrr}vr^2 + Y_{\delta}\cos\ \delta \end{aligned} \tag{5}$$

$$N_H = N_{\dot{v}}\dot{v} + N_{\dot{r}}\dot{r} + N_v v + N_r r + N_{vvv}v^3 + N_{rrr}r^3 + N_{vvr}v^2 r + N_{vrr}vr^2 + + N_\delta \cos\ \delta \tag{6}$$

where $X(u)$ is for instance, the velocity dependent damping function. This model does not involve modelling the rudder and propeller. In this study the hull derivatives are of prime interest and the effect of rudder and propeller can be brought in by some empirical relationships when required (trajectory simulation). Bilge keels have not been considered in this work.

3 Planar Motion Mechanism Tests

The Horizontal Planar Motion Mechanism (HPMM) is a device developed to determine the surface ships velocity and acceleration dependent derivatives for the sway and yaw modes. This results to be the most promising method among all the existing captive model test methods for the determination of hydrodynamic derivatives, as it contains all the derivatives defined in the mathematical model [Eqs. (4)–(6)] and contributing to the equations of motion [13, 14].

3.1 General Experimental Procedure

The HPMM consists of 2 oscillators, one of which produces a transverse oscillation at the bow and the other at the stern, while the model moves down the towing tank with a constant towing carriage velocity in the current procedure. The in-phase oscillations of the oscillators in transverse direction to the towing tank longitudinal axis produces pure sway motion of the model, while the out of phase oscillation brings in the pure yaw motion. The model pure yaw motion, initially subjected to a certain drift angle, brings together the drift and yaw motion. The model velocity is always tangential to the oscillating path. In each mode, the forces and moments acting on the model are measured and resolved using the special transducers and instrumentation. Hydrodynamic derivatives can then be determined from the measured forces and moments by using either a higher order curve-fit method or Fourier series expansion method.

3.2 Problem Formulation

The problem formulation has been tedious, as did involve a laborious procedure of many trials in order to arrive at the expressions for the body oscillations model, so that they in turn yield the most simplified expressions for the calculation of

hydrodynamic derivatives. The Fourier series expansion method has been used for the determination of the derivatives and according to it the hydrodynamic forces and moments acting on the ship hull can be expressed as defined in Eq. (7a):

$$\text{Hydrodynamic force/moment} = \sum_{m=0}^{\infty} (a_m \cos\ m\omega t + b_m \sin\ m\omega t) \tag{7a}$$

where the Fourier coefficients are given by Eq. (7b):

$$a_0 = \frac{1}{T}\int_0^T f(t)dt \quad a_m = \frac{2}{T}\int_0^T f(t)\cos\ m\omega t dt \quad b_m = \frac{2}{T}\int_0^T f(t)\sin\ m\omega t dt \tag{7b}$$

in which, a truncated series up to 3rd harmonics is chosen, because the mathematical model considers only up to the 3rd order terms. Considering an arbitrary phase angle (γ) at the start value of oscillation, the above trigonometric function can be written as set in Eq. (7c)

$$\begin{aligned} \cos\ m\omega t &= \cos m(\omega t+\gamma)\cos m\gamma + \sin m(\omega t+\gamma)\sin m\gamma \\ \sin\ m\omega t &= \sin m(\omega t+\gamma)\cos m\gamma - \cos m(\omega t+\gamma)\sin m\gamma \end{aligned} \tag{7c}$$

Hence, the hydrodynamic force/moment can now be expresses as follows in the Eq. (7d)

$$\begin{aligned} H_M = \sum_{m=0}^{\infty} \{ & a_{dMm}(\cos\ m(\omega t+\gamma)\cos\ m\gamma + \sin\ m(\omega t+\gamma)\sin\ m\gamma) \\ & + b_{dMm}(\sin\ m(\omega t+\gamma)\cos\ m\gamma - \cos\ m(\omega t+\gamma)\sin\ m\gamma)\} \end{aligned} \tag{7d}$$

where H = *X*, *Y*, *N*; *d* = *x*, *y*, *n*; *M* = *Y*, *N*, *YN*; *m* = 1, 2, 3.

x represents the direction of surge force, y represents the direction of sway force, *n* represents yaw moment about z axis, *Y* represents pure sway mode, *N* represents pure yaw mode, *YN* represents combined mode and *m* represents the harmonics of Fourier series.

3.2.1 Pure Sway Mode

This part of HPMM comprises oscillating the model in transverse direction in which the oscillators fixed on the model oscillate in phase and the model kinematics parameters are represented as:

$$\text{Transverse displacement,} \qquad y_0 = -y_{0a} \sin \omega t = y \tag{8}$$

$$\text{Transverse velocity,} \qquad \dot{y}_0 = -y_{0a}\omega \cos \omega t = v \tag{9}$$

$$\text{Transverse acceleration,} \qquad \ddot{y}_0 = y_{0a}\omega^2 \sin \omega t = \dot{v} \tag{10}$$

$$\text{Forward velocity,} \qquad u_0 = V = u \tag{11}$$

$$\text{Forward acceleration,} \qquad \dot{u} = 0 \tag{12}$$

Yaw angular displacement, velocity and acceleration,

$$\psi = r = \dot{r} = 0 \tag{13}$$

In pure sway mode oscillations, the mathematical model given by Eqs. (4)–(6) will have only sway motion dependent terms and thus they reduce to:

$$X_{HY} = X_{u|u|}u|u| + X_{vv}v^2 \tag{14}$$

$$Y_{HY} = Y_{\dot{v}}\dot{v} + Y_v v + Y_{vvv}v^3 \tag{15}$$

$$N_{HY} = N_{\dot{v}}\dot{v} + N_v v + N_{vvv}v^3 \tag{16}$$

Expanding the hydrodynamic reaction forces and moment with applying Fourier series and substituting Eqs. (8)–(11) in Eqs. (14)–(16), and comparing the like terms in the corresponding equations by putting $r = 0$, we obtain the derivatives for the pure sway defined in Eqs. (17)–(24):

$$X_{vv} = \frac{2}{y_{0a}^2\omega^2} a_{xY2} \tag{17}$$

$$X_{u|u|} = \frac{1}{V^2}\left[a_{xY0} - a_{xY2}\right] \tag{18}$$

$$Y_{\dot{v}} = \frac{1}{y_{0a}\omega^2} b_{yY1} \tag{19}$$

$$Y_{vvv} = \frac{-4}{y_{0a}^3\omega^3} a_{yY3} \tag{20}$$

$$Y_v = \frac{1}{y_{0a}\omega}\left[3a_{yY3} - a_{yY1}\right] \tag{21}$$

$$N_{\dot{v}} = \frac{1}{y_{0a}\omega^2} b_{nY1} \tag{22}$$

$$N_{vvv} = \frac{-4}{y_{0a}^3 \omega^3} a_{nY3} \tag{23}$$

$$N_v = \frac{1}{y_{0a}\omega}[3a_{nY3} - a_{nY1}] \tag{24}$$

3.2.2 Pure Yaw Mode

In HPMM experiment, the oscillators are made to oscillate with a predetermined phase difference in order to take into account a rotation in the horizontal plane. In the present numerical model, the pure yaw mode is achieved by oscillating the vessel about z-axis, and at the desired frequency. The yaw acceleration causes a fluctuation in surge velocity. At any instant, the velocity will be tangential to the oscillating path. In model tests this condition is used for deriving the expression for the phase angle, which is not required for the numerical simulation The model kinematic parameters are represented as

$$\text{Yaw angle,} \qquad \psi = -\psi_a \cos\ \omega t \tag{25}$$

$$\text{Yaw rate,} \qquad \dot{\psi} = r = r_a \sin\ \omega t \tag{26}$$

$$\text{Yaw acceleration,} \qquad \ddot{\psi} = \dot{r} = r_a \omega\ \cos\ \omega t \tag{27}$$

$$\text{Forward velocity,} \quad u = \sqrt{(V^2 + \dot{y}_0^2)} = u_{cN} + u_{aN} \cos\ 2\omega t \tag{28}$$

$$\text{Forward acceleration,} \qquad \dot{u} = -2u_{aN}\omega \sin\ 2\omega t \tag{29}$$

$$\text{Sway displacement velocity and acceleration,} \quad y = v = \dot{v} = 0 \tag{30}$$

where

$$u_{aN} = \frac{y_{0a}^2 \omega^2}{4V} \quad \text{and} \quad u_{cN} = V + u_{aN}$$

In pure yaw mode oscillations, the mathematical model given by Eqs. (4)–(6) have only yaw motion dependent terms. Hence these equations are simplified to:

$$X_{HN} = X_{\dot{u}}\dot{u} + X_{uu}u|u| + X_{rr}r^2 \tag{31}$$

$$Y_{HN} = Y_{\dot{r}}\dot{r} + Y_r r + Y_{rrr}r^3 \tag{32}$$

$$N_{HN} = N_{\dot{r}}\dot{r} + N_r r + N_{rrr} r^3 \tag{33}$$

By expanding the hydrodynamic reaction forces and moment in Fourier series, and substituting Eqs. (25)–(29) in Eqs. (31)–(33) and following up by comparing like terms in the corresponding equations by putting $v = 0$, we get the derivatives of the pure yaw defined in Eqs. (34)–(41):

$$X_{\dot{u}} = \frac{-1}{2u_{aN}} b_{xN2} \tag{34}$$

$$X_{rr} = \frac{2}{r_a^2}\left[\frac{2u_{cN}u_{aN}}{V^2}(a_{xY0} - a_{xY2}) - a_{xN2}\right] \tag{35}$$

$$Y_{\dot{r}} = \frac{1}{r_a \omega} a_{yN1} \tag{36}$$

$$Y_{rrr} = \frac{-4}{r_a^3}\left[\frac{b_{xN2} r_a}{4\omega} + b_{yN3}\right] \tag{37}$$

$$Y_r = \frac{1}{r_a}\left[b_{yN1} + \frac{b_{xN2} r_a}{2u_{aN}\omega}(u_{cN} - \frac{u_{aN}}{2}) + 3\left(\frac{b_{xN2} r_a}{4\omega} + b_{yN3}\right)\right] \tag{38}$$

$$N_{\dot{r}} = \frac{1}{r_a \omega} a_{nN1} \tag{39}$$

$$N_{rrr} = \frac{-4}{r_a^3} b_{nN3} \tag{40}$$

$$N_r = \frac{1}{r_a}[b_{nN1} + 3b_{nN3}] \tag{41}$$

3.2.3 Combined Motion

In this mode the combined sway and yaw motions are induced upon the model by producing yaw motion on a drifted model and repeating the procedure for various drift angles in the experiment. In a numerical simulation both sway and yaw oscillations can be simultaneously imposed on the model. The kinematic parameters of the model in earth-fixed co-ordinate system are transformed to ship fixed co-ordinate system using ψ:

$$u = V\ \cos\ \psi + \dot{y}_0 \sin\ \psi \tag{42}$$

$$v = -V\ \sin\ \psi + \dot{y}_0 \cos\ \psi \tag{43}$$

we consider,

$$\psi \leq 12^{\circ}; \text{then}\ \cos\ \psi = 1; \sin\ \psi = \psi \tag{44}$$

$$u = u_{cYN} + u_{aYN} \cos\ 2\omega t \tag{45}$$

$$\dot{u} = -2u_{aYN}\omega \sin\ 2\omega t \tag{46}$$

$$v = v_{aYN} \cos\ \omega t \tag{47}$$

$$\dot{v} = -v_{aYN}\omega \sin\ \omega t \tag{48}$$

where $v_{aYN} = V\psi_a - y_{0a}\omega$, $u_{aYN} = \frac{y_{0a}\omega\psi_a}{2}$ and $u_{cYN} = V + u_{aYN}$.

The yaw motion equations remain same, due to the pure yaw mode as defined in Eqs. (25)–(27), for the both earth-fixed and ship-fixed co-ordinate systems. As the model undergoes combined sway and yaw mode oscillations, the mathematical model defined by Eqs. (4)–(6) have both sway and yaw motion dependent terms. Hence,

$$X_{HYN} = X_{\dot{u}}\dot{u} + Y_{\dot{v}}vr + X_u(u) + X_{vr}vr + X_{vv}v^2 + X_{rr}r^2 \tag{49}$$

$$Y_{HYN} = X_{\dot{u}}ur + Y_{\dot{v}}\dot{v} + Y_{\dot{r}}\dot{r} + Y_v v + Y_r r + Y_{vvv}v^3 + Y_{rrr}r^3 + Y_{vvr}v^2 r + Y_{vrr}vr^2 \tag{50}$$

$$N_{HYN} = N_{\dot{v}}\dot{v} + N_{\dot{r}}\dot{r} + N_v v + N_r r + N_{vvv}v^3 + N_{rrr}r^3 + N_{vvr}v^2 r + N_{vrr}vr^2 \tag{51}$$

By expanding the hydrodynamic forces and moments in Fourier series and substituting Eqs. (25)–(27) and (45)–(48) in Eqs. (49)–(51) and comparing the like terms in the corresponding equations putting $\gamma = 0$, we get the derivatives in combined motion given by the Eqs. (52)–(56):

$$X_{vr} = \frac{2}{v_{aYN}r_a} b_{xYN2} - \frac{b_{yY1}}{y_{0a}\omega^2} - b_{xN2}\frac{u_{aYN}}{u_{aN}} \tag{52}$$

$$Y_{vvr} = \frac{4}{v_{aYN}^2 r_a}\left[b_{yYN3} - \frac{b_{xN2}r_0}{4\omega}\left(\frac{u_{aYN}}{u_{aN}} + 1\right) - b_{yN3}\right] \tag{53}$$

$$Y_{vrr} = \frac{-4}{v_{aYN}r_a^2}\left[a_{yYN3} + a_{yY3}\left(\frac{v_{aYN}}{v_a}\right)^3\right] \tag{54}$$

$$N_{vvr} = \frac{4}{v_{aYN}^2 r_a}[b_{nYN3} - b_{nN3}] \tag{55}$$

$$N_{vrr} = \frac{-4}{v_{aYN} r_a^2}\left[a_{nYN3} + a_{nY3}\left(\frac{v_{aYN}}{v_a}\right)^3\right] \tag{56}$$

A detailed experimental procedure for carrying out model tests is explained in [15].

3.3 HPMM Numerical Simulations

Numerical methods are more flexible and thus numerous design versions can be analysed. They are efficient in performing simulations, analysing results through flow visualizations and creating related animations. Every small detail of flow patterns can be easily obtained spotting it any location around the ship hull, which may not be possible while conducting experiments. In model tests, such as the free-running tests are, it might be very easy to study the influence of appendages on the manoeuvrability of the vessel while in the numerical modelling the ship with appendages is a tedious task to create it. Once this is overcome, the rest of the processes can result simpler than experiments.

The HPMM simulation requires a numerical computational domain and a solver capable of solving the fluid flow equations, while the mesh in the fluid domain is re-oriented due to the hull motion. ANSYS ICEM CFD has been used for the mesh generation and the dynamic mesh motion option of the commercial CFD package ANSYS CFX has made possible to bring in the prescribed ship body motion.

3.3.1 Grid System

In the present work a structured grid system with hexahedral cells has been used with near wall refinement. The meshing has been carried out in ANSYS ICEM CFD. In order to avoid the near-wall deformation of the elements, the interface meshing strategy has been adopted, where the ship hull moves within an inner computational domain. CFX uses a ‘mesh morphing’ model that calculates the new node positions at each time step, while maintaining the basic mesh topology. However, the nodal displacements are calculated by using a spring analogy method. The outer and inner computational domains have a common merged interface and fluxes are transferred across it, keeping intact the near-wall mesh around the ship model. In order to avoid the complexity of sharp corners, a cylindrical inner domain with circular faces has been applied. This type of meshing strategy also helps in capturing the free-surface effects. The outer domain extends 1.5 L from the aft, 0.8 L from the bow, 1 L from each of port and star board sides and the bottom

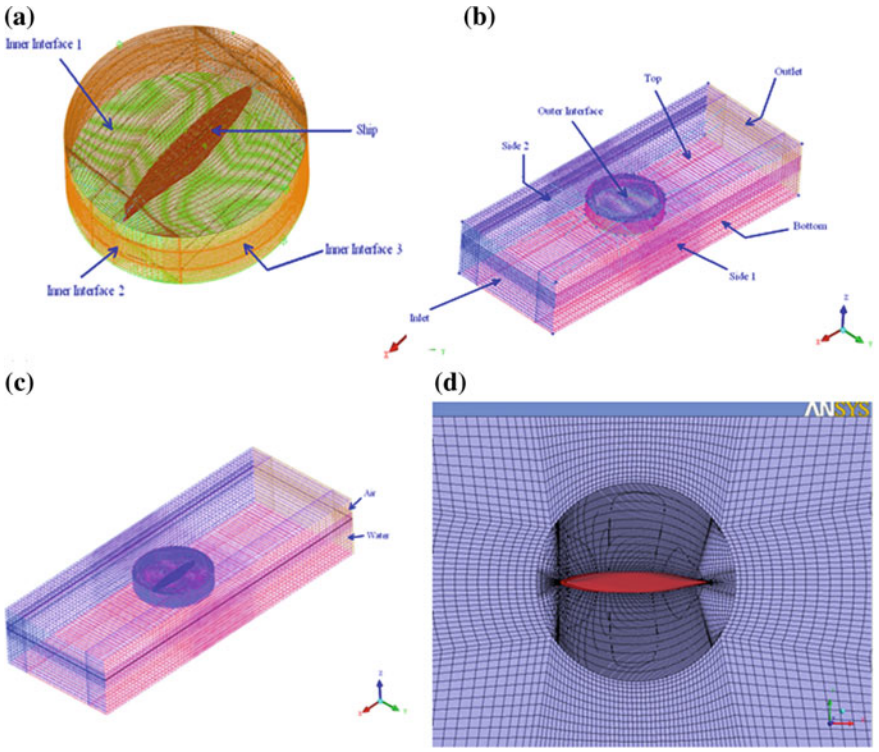

Fig. 3 3-dimensional structured grid system. **a** Inner domain, **b** outer domain, **c** combined domain and **d** mesh cut plane from the top

extends 0.6 L from the keel indicating the deep water conditions. The generated mesh has 0.6 million hexahedral cells. A more refined mesh couldn't be used because of both, computational time and resource constraints. The above described mesh is shown in Fig. 3.

3.3.2 Turbulence Model, Boundary Conditions and Solver Settings

The 2-equations k-ω shear stress transport (SST) model has been used for the calculations, by making use of wall and boundary distance formulations [16]. As a result, the near wall regions are well resolved ($y^+ < 2$).

No-slip wall boundary condition has been imposed on the ship hull, side and bottom boundaries [17]. Since the boundaries have been chosen sufficiently far away from the hull, it was assumed that there are no interactions between these boundaries due to viscous flow past them. The free-stream conditions prevail on the top. An inlet flow velocity of 1 m/s has been imposed at the inlet boundary for both air and water and the flow leaves the outlet with outflow conditions. The outer and

inner interfaces have been merged to a single one and interface boundary condition has been assigned to it.

The space and time discretization use the high resolution and second order backward Euler schemes, respectively. A homogeneous coupled Volume Of Fluid (VOF) method has been adopted for capturing the free-surface effects. For convergence limiter, the RMS values have been set to a target value of 10^{-5}.

3.3.3 Simulations

Grid independency has not been carried out, but it has been well ensured that the grid is capable enough of producing reliable results. Steady state simulations have been initially carried out with objective to obtain converged results, and to initialize the mesh motions. The drag force on the ship hull has been found to match well with experimental and theoretical values. In order to carry out the HPMM tests in a numerical towing tank, ship body along with the inner domain has been subjected to pure sway, pure yaw and combined sway and yaw sinusoidal motions. The air and water flow velocity are taken as 1.0 m/s. Table 2 shows the values of various simulation constants. Motions have been brought in by using the transformations (translation and rotation) of co-ordinate axes, and the simulations time step has been calculated as 0.01 s. Since the solution follows an implicit scheme, the time step is not of major concern. The Courant number has been fixed to 0.5 and a smallest cell size to be 0.02 m in the flow direction. At each time step the mesh is updated with respect to its position obtained at the previous time step.

3.3.4 Pure Sway

The transverse motion of the ship along with the inner domain has been accomplished using the sinusoidal function given in Eq. (8). The mesh motions have been accomplished using the following translation of co-ordinate axes in CFX.

Table 2 Simulation constants

Constants	Values
T	13.33 s
ω	0.4714 rad/s
ω'	2.28
V	1 m/s
y_{0a}	0.3 m
y'_{0a}	0.0617
$\psi_a = \psi'_a$	0.19 rad
Re	4.86×10^6
Fr	0.145
β_a	12°

$$[x' \quad y' \quad z']^T = [x \quad (y + y_0) \quad z]^T \tag{59}$$

3.3.5 Pure Yaw

In order to rotate the ship model and the inner domain about z-axis, the sinusoidal function, see Eq. (25), has been used. The mesh motions have been accomplished by using the following rotation of co-ordinate axes in CFX.

$$\begin{Bmatrix} x' \\ y' \\ z' \end{Bmatrix} = \begin{Bmatrix} x \cos \psi + y \sin \psi \\ -x \sin \psi + y \cos \psi \\ z \end{Bmatrix} \tag{60}$$

3.3.6 Combined Sway and Yaw

The mesh motions in this case are the superimposition of the above 2 cases and the resulting transformations in CFX are shown in Eq. (61):

$$\begin{Bmatrix} x' \\ y' \\ z' \end{Bmatrix} = \begin{Bmatrix} x \cos \psi + y \sin \psi \\ -x \sin \psi + y \cos \psi + y_0 \\ z \end{Bmatrix} \tag{61}$$

4 Results and Discussions

The solution process has been carried out for 3 cycles in and for all 3 modes- pure sway, pure yaw and combined motions. The mesh displacements and pressure distributions around the hull for extreme motions have been shown in Figs. 4, 5 and 6. The first cycle has shown higher values with lots of fluctuations due to transience. The 2nd and 3rd cycles have shown constant trends with same maximum values. This is demonstrated as shown in Fig. 7. Hence the 3rd cycle was chosen for the analysis, as CFX uses a global reference frame for the calculations that does not move with the body. The conversion of the applied axes system to ship-fixed counterpart is almost impossible with CFX. Since the formulations had been with respect to Ship-Fixed Co-ordinate System (SFCS), the corresponding transformations have been done through a MATLAB code, where the time history of a force/moment has been calculated in both the co-ordinate systems taken from experiments for setting the hydrodynamic derivatives and assumed body motions. The difference between the values in these 2 co-ordinate systems have been finally subtracted from the corresponding CFD results. These kind of transformations are

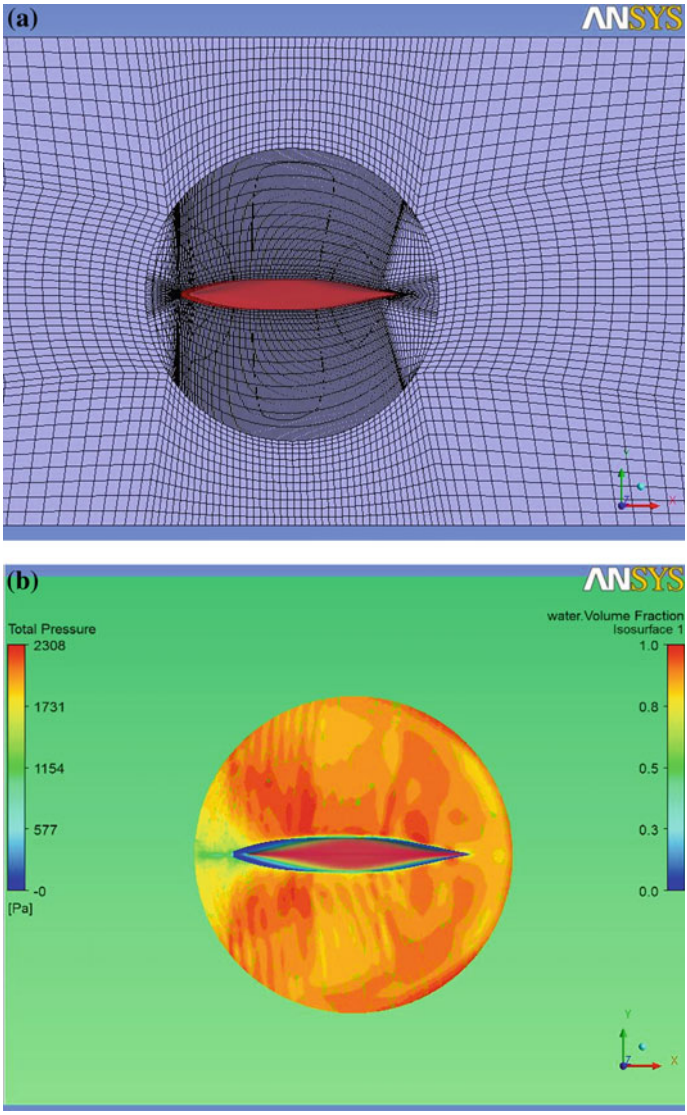

Fig. 4 Extreme sway motion. **a** Mesh displacement and **b** total pressure distribution around the hull

required in cases where the rotations of the co-ordinate system is involved and thus, no transformations were required for pure-sway case.

Section 3.2 shows the complete formulation of the problem and the derivation of the expressions for the calculation of the hydrodynamic derivatives. All the expressions for hydrodynamic derivatives have been defined in Eqs. (17)–(24),

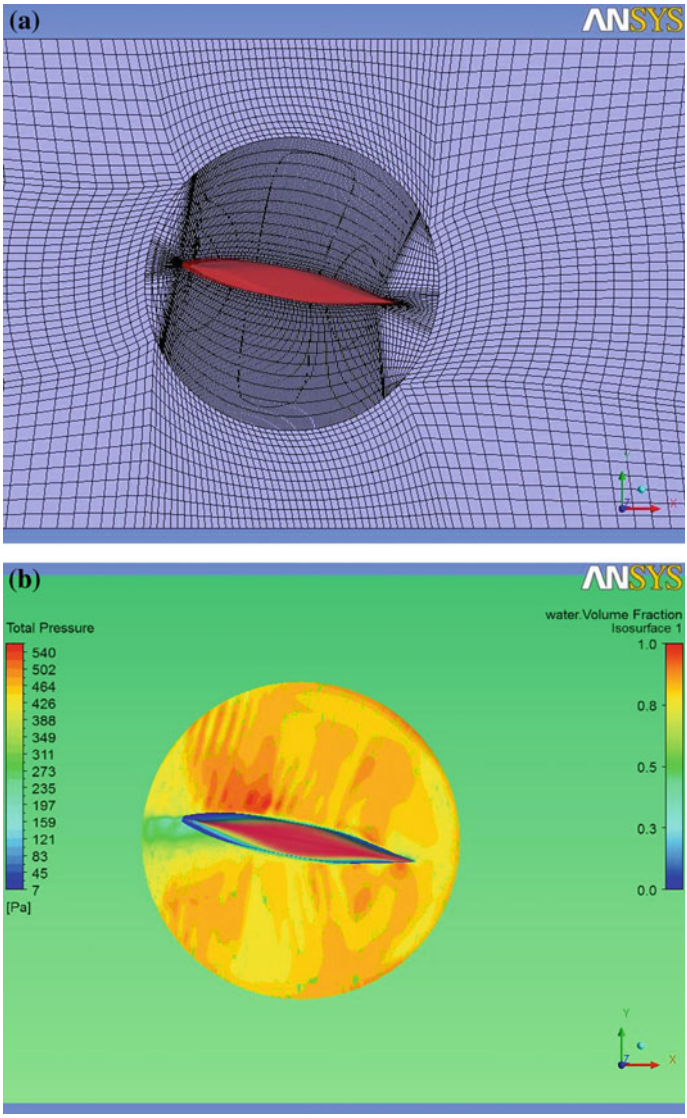

Fig. 5 Extreme yaw motion. **a** Mesh displacement and **b** total pressure distribution around the hull

Eqs. (34)–(41) and Eqs. (52)–(56) and have been expressed in terms of Fourier constants and hence, their evaluation required as influence a lot the simulations results. It is important to mention, that they have been obtained by the numerical integration of the time histories of forces and moments over a cycle using Simpson's rule or by obtaining the definite integral of the equation of the fitted

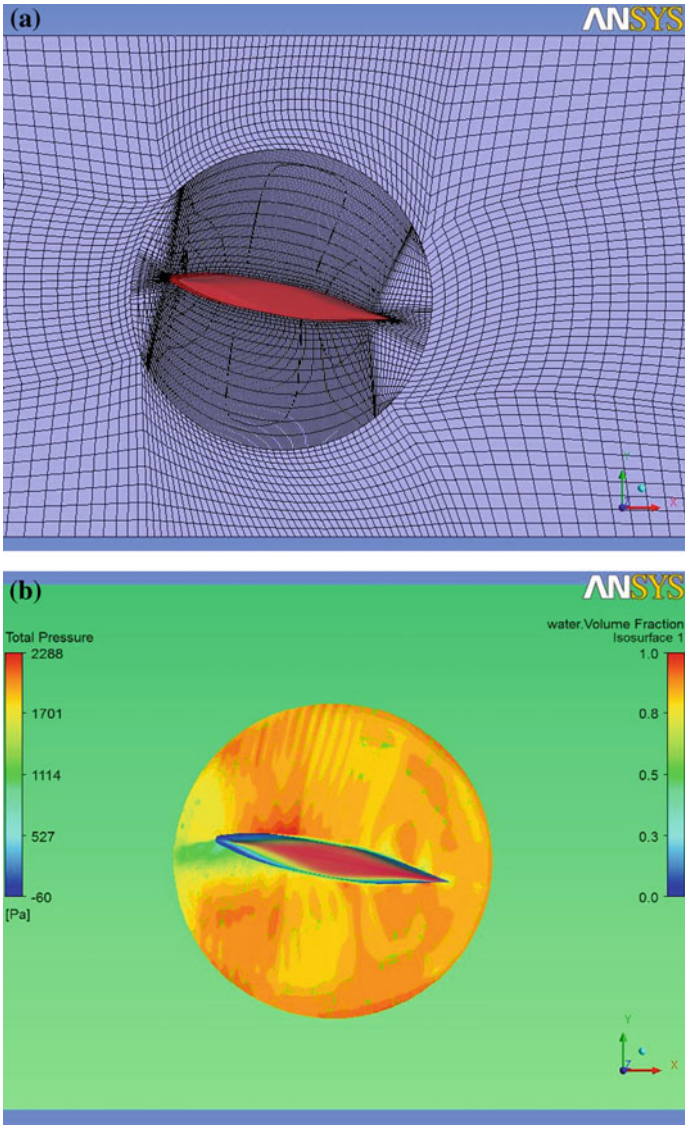

Fig. 6 Extreme combined motion. **a** Mesh displacement and **b** total pressure distribution around the hull

curve, as a function of time. The derivatives for the model have been obtained in the dimensional form initially, and then made non-dimensional to ease their representation. The non-dimensional factors for forces and moment are $\frac{1}{2}\rho L^2 V^2$ and $\frac{1}{2}\rho L^3 V^2$, respectively. Figures 8, 9 and 10 show the force and moment time histories in each mode of mesh motion. These figures show that the obtained numerical

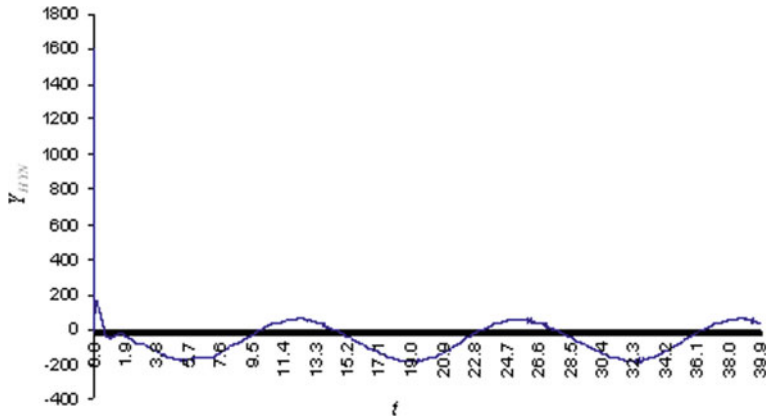

Fig. 7 Three cycles of combined motion simulation

simulations results do not represent a smooth curve, at each time step. Thus, it is appropriate to fit a smooth curve in order to obtain the Fourier constants accurately. As a relatively coarse mesh has been used, the values of forces and moments do not represent a very smooth curve at various time steps. The spikes must be eliminated and need to be replaced with interpolated values by using the values from previous and later time steps. However, some of them contribute towards higher order terms too. These values have been retained as they are. The Fourier coefficients have been obtained from the numerical integration of the curves. The experience has shown that Fourier coefficients are accurately predicted when smoother curves are used for integration.

Table 3 shows the values of hydrodynamic derivatives calculated through the presented method, as adopted in this chapter and their comparison with published experimental values [11] are given. The derivatives have an assigned symbols depending on their relative importance [18] for the trajectory prediction and stability characteristics. The forces and moments obtained through CFD simulations are smoothened and have been transformed into ship-fixed coordinate system (sfcs) and they have been compared with theoretical time histories and corresponding to the experimental values for hydrodynamic derivatives in sfcs. The deviations are found not very high. Since the forces and moments have been predicted well, it is implied that the derivatives have been also well predicted. The numerical simulations of HPMM using RANSE based CFD methods has been found to work well at least for moderate motion amplitudes. The Fourier series expansion method or the harmonic analysis, used in this work, for defining derivatives is indeed a promising, and has been successful enough to define all the 21 derivatives-coupled, uncoupled and cross-coupled, as required by the mathematical model. In the present case, the deviations with respect to the experimental results are found to follow a particular pattern. The uncoupled derivatives have been observed to be well predicted (0.8–6%). The coupled ones show more deviation (5–11%) and the cross-coupled

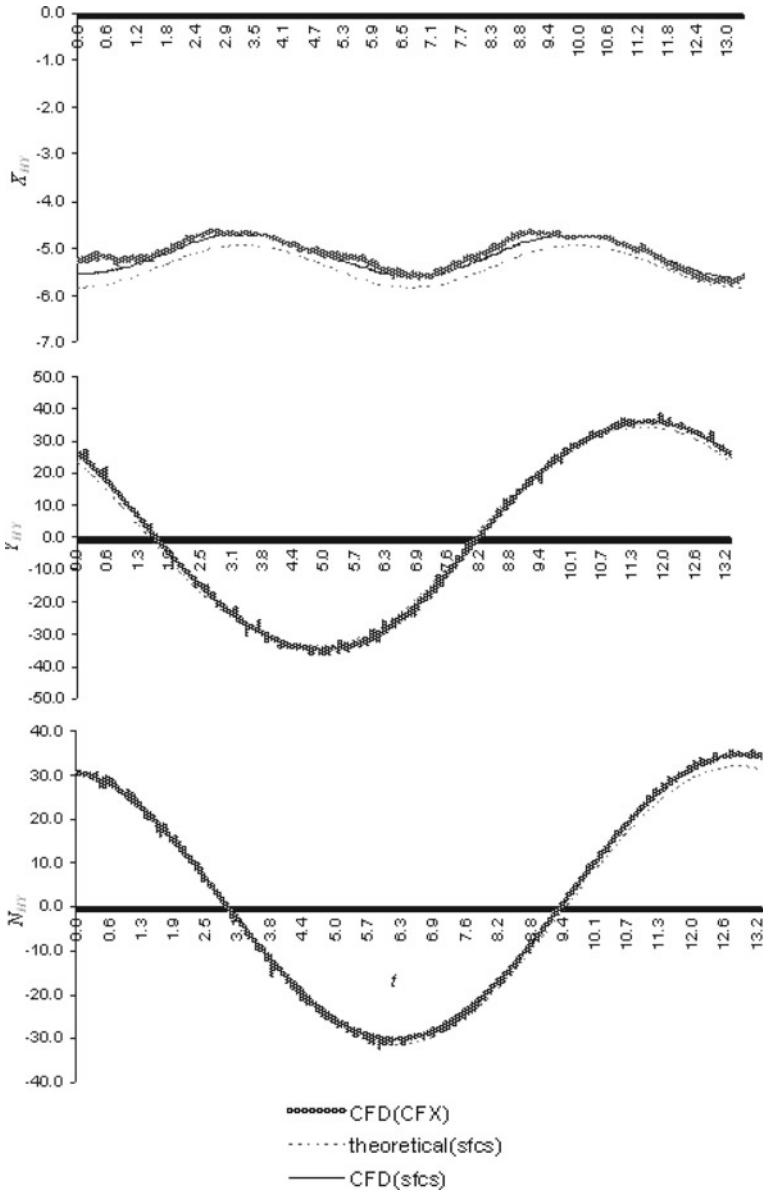

Fig. 8 Time histories of forces and moment in pure sway

show furthermore deviation (10–12%). The reason might be due to the relative coarseness of the mesh, for which the coupling effect of body motions and fluid flow has been not very well captured. However, the improvements might be possible applying better refinement techniques for meshing.

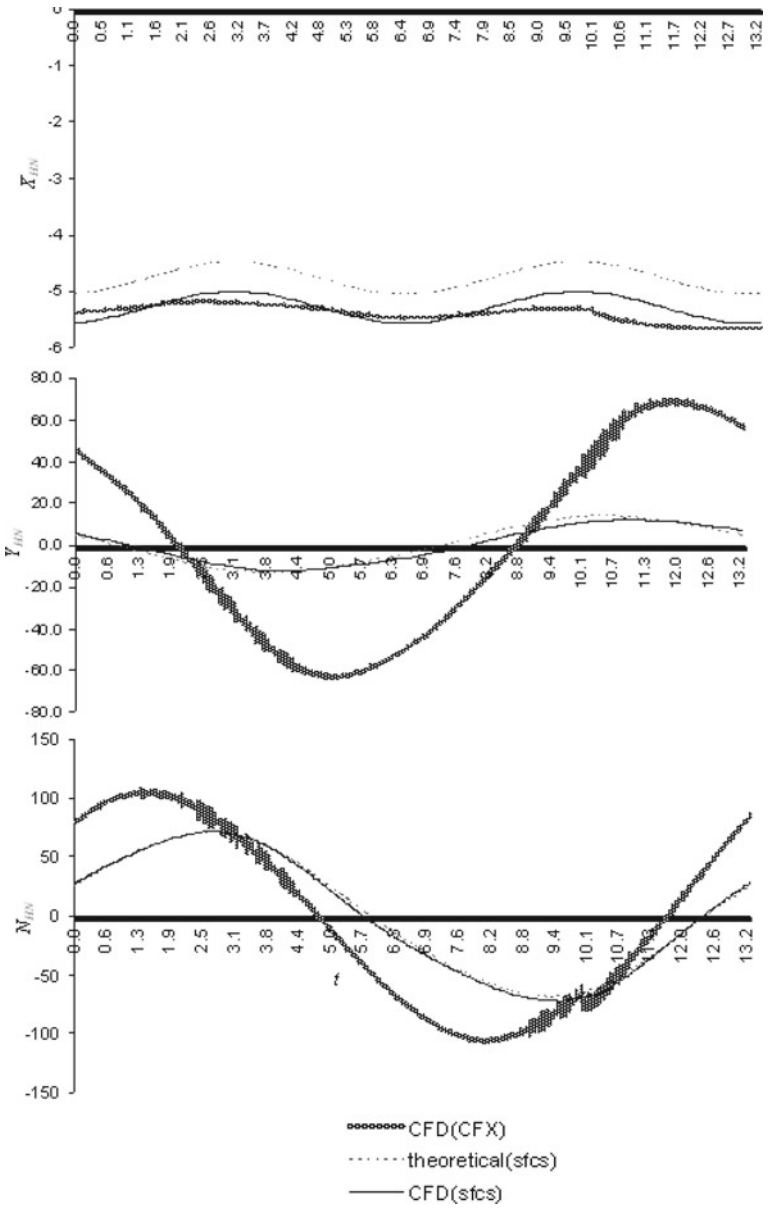

Fig. 9 Time histories of forces and moment in pure yaw

The variables assigned to the derivatives in assessing their relative importance in Table 3 indicates that the most of the derivatives with higher relative importance have been well predicted. As manoeuvring is concerned with low frequency,

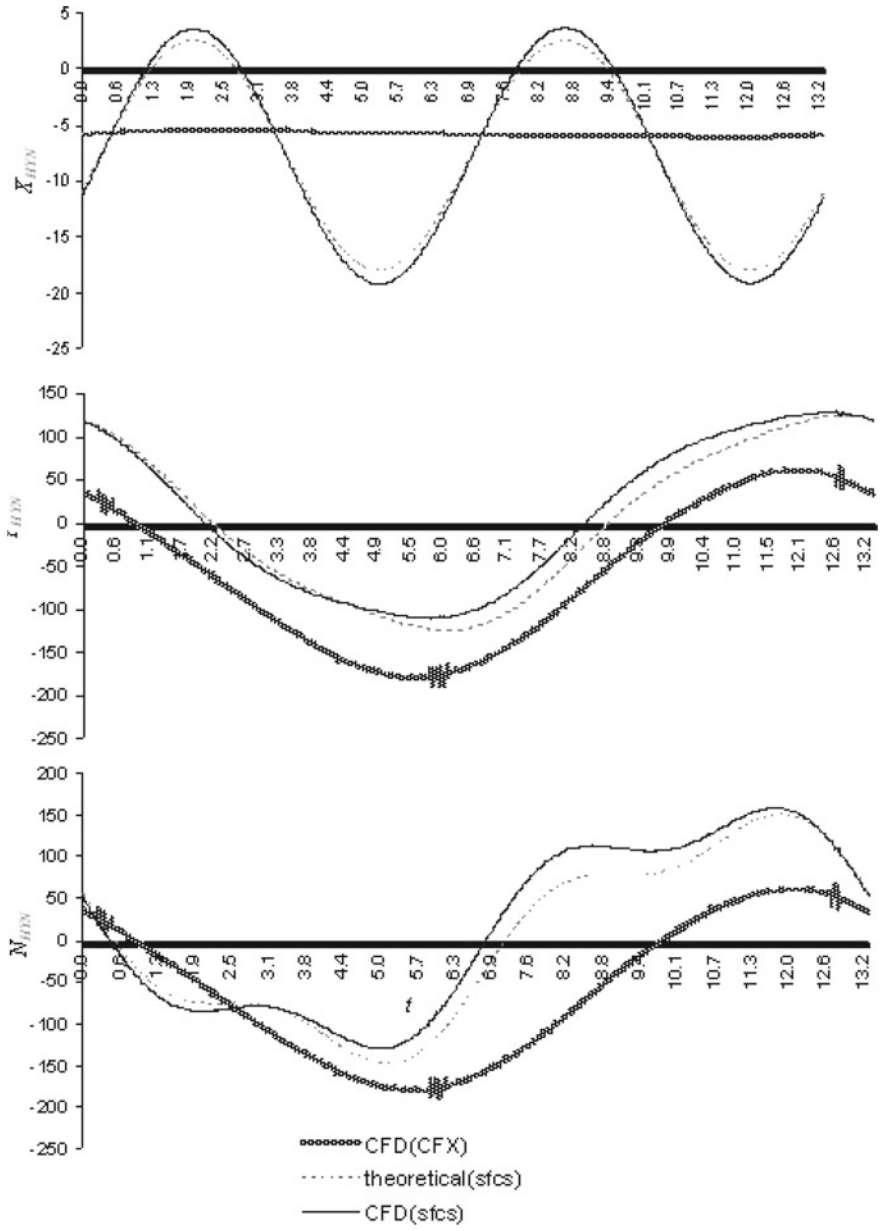

Fig. 10 Time histories of forces and moment in combined motion

the frequency of oscillation has been restricted to be at lowest possible level. Further frequency lowering has been found to result in unwanted oscillations in the time traces.

Table 3 Hydrodynamic coefficients in manoeuvring

Hyd. deri.	Non-dim. factor	Type	Present CFD	Expt. [11]	Deviation (%)	Category [18]
$X'_{\dot{u}}$	$0.5\rho L^3$	Uncoupled	−0.00025	−0.00024	4.16	*A*
$X'_{u\|u\|}$	$0.5\rho L^2$	,,	−0.00044	−0.00042	4.76	*A*
X'_{vv}	$0.5\rho L^2$	Coupled	−0.00365	−0.00386	−5.44	*C*
X'_{rr}	$0.5\rho L^4$	,,	0.00021	0.0002	5.01	*C*
X'_{vr}	$0.5\rho L^3$	Cross-coupled	−0.00345	−0.00311	10.93	*D*
$Y'_{\dot{v}}$	$0.5\rho L^3$	Uncoupled	−0.00699	−0.00705	−0.8	*A*
Y'_{v}	$0.5\rho L^2 V$	,,	−0.0118	−0.0116	1.7	*A*
Y'_{vvv}	$0.5\rho L^2 V$	,,	−0.111	−0.109	1.8	*C*
$Y'_{\dot{r}}$	$0.5\rho L^4$	Coupled	−0.000372	−0.00035	6.57	*A*
Y'_{r}	$0.5\rho L^3 V$	Coupled	0.00264	0.00242	9.01	*A*
Y'_{rrr}	$0.5\rho L^5/V$	Coupled	0.00192	0.00177	8.47	*D*
Y'_{vvr}	$0.5\rho L^3/V$	Cross-coupled	0.0239	0.0214	11.68	*A*
Y'_{vrr}	$0.5\rho L^4/V$	,,	−0.0507	−0.0405	10.09	*D*
$N'_{\dot{v}}$	$0.5\rho L^4$	Coupled	−0.000384	−0.00035	9.71	*A*
N'_{v}	$0.5\rho L^3 V$	,,	−0.00421	−0.00385	9.35	*A*
N'_{vvv}	$0.5\rho L^3/V$	,,	0.00166	0.001492	11.41	*C*
$N'_{\dot{r}}$	$0.5\rho L^5$	Uncoupled	−0.000408	−0.00042	−2.85	*A*
N'_{r}	$0.5\rho L^4 V$	,,	−0.00234	−0.00222	5.41	*A*
N'_{rrr}	$0.5\rho L^6/V$	,,	−0.00241	−0.00229	5.24	*D*
N'_{vvr}	$0.5\rho L^4/V$	Cross-coupled	−0.0471	−0.0424	11.08	*A*
N'_{vrr}	$0.5\rho L^5/V$	Cross-coupled	0.00175	0.00156	12.17	*D*

A—Derivatives deemed of major importance
C—Derivatives deemed of minor importance
D—Derivatives deemed negligible

Since most of the important derivatives have been predicted well, the trajectories do not deviate much from the actual trajectory in definitive manoeuvres. This fact has been illustrated using Fig. 11. A program has been developed in MATLAB for the numerical integration (4th order Runge-Kutta method) of the equations of motions represented by the mathematical model of Son and Nomoto [11]. Two manoeuvres have been simulated (1) turning circle and (2) zig-zag manoeuvres. From Fig. 11a, b, it is evident that the trajectories have been predicted quite well by using the presented CFD simulation approach.

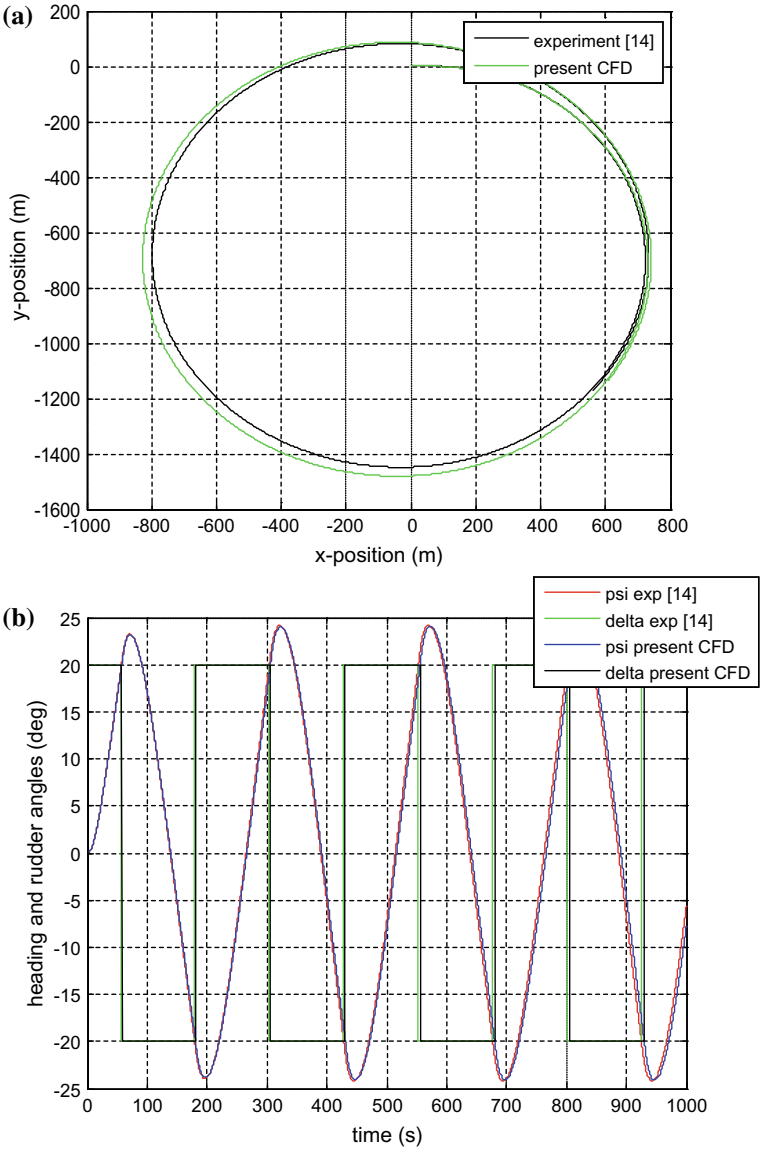

Fig. 11 Simulated trajectory of the vessel. **a** Turning circle manoeuvre for 35° rudder angle and **b** 20/20 zig-zag manoeuvre

5 Conclusions

The Fourier series expressions formulated here for the calculation of hydrodynamic derivatives can be used for any ship numerical simulations, provided that the time histories of forces and moments are obtained through simulations or model testing. The present work finds RANSE based CFD, as a promising alternative in the determination of all the hydrodynamic derivatives required in a mathematical model and hence can be considered as a reliable tool in the manoeuvrability assessment of vessels, especially useful for the early ship design phase. On the whole, this work finds its success in exploring and exploiting various features of a general-purpose fluid flow solver to solve a non-linear dynamic ship manoeuvring problem.

References

1. Toxopeus SL (2009) Deriving mathematical maneuvering models for bare ship hulls using viscous flow calculations. J Mar Sci Technol 14:30–38
2. Carrica PM, Stern F (2008) DES simulations of KVLCC1 in turn and zig-zag maneuvers with moving propeller and rudder. In: SIMMAN workshop on verification and validation of ship maneuvering simulation methods, pp F11–F16
3. Janardhanan S, Krishnankutty P (2009) Numerical estimation sway-dependent non-linear hydrodynamic derivatives in surface-ship maneuvering. In: Proceedings of the third international conference in ocean engineering, Chennai, India
4. Nonaka K, Miyazaki H, Nimura T, Ueno M, Hino T, Kodama Y (2007), Calculation of hydrodynamic forces acting on a ship in maneuvering motion. In: Research paper. Ship Research Institute, Japan, pp 307–317
5. Sulficker N (2007) RANSE based estimation of hydrodynamic forces acting on ships in dynamic conditions. M.S. thesis, Department of Ocean Engineering, IIT Madras, pp 50–82
6. Cura-Hochbaum A (2006) Prediction of hydrodynamic coefficients for a passenger ship model. In: International conference in marine hydrodynamics, pp 933–942
7. Cura-Hochbaum A, Vogt M, Gatchell S (2008) Maneuvering prediction for two tankers based on RANS simulations. In: SIMMAN workshop on verification and validation of ship maneuvering simulation methods, pp F23–F28
8. Xing-Kaeding Y, Jensen AG (2006) Simulation of ship motions during maneuvers. Ship Technol Res Schiffstechnick 53(4):14–28
9. Tyagi A, Sen D (2006) Calculation of transverse hydrodynamic coefficients using computational fluid dynamic approach. Ocean Eng 33:798–809
10. Ohmori T (1998) Finite-volume simulation of flows about a ship in maneuvering motion. J Mar Sci Technol 3:82–93
11. Son KH, Nomoto K (1981) On the coupled motion of steering and rolling of a high speed container ship. J Soc Naval Archit Jpn 150:73–83
12. Abkowitz MA (1964) Testing techniques used for the measurement of hydrodynamic derivatives. In: Lectures on ship hydrodynamics—steering and manoeuvrability, pp 53–62
13. Bishop RED, Parkinson AG (1970) On the planar motion mechanism used in ship model testing. Philos Trans Royal Soc Lond Ser A Math Phys Sci 266(1171):35–61
14. Crane CL, Eda H, Landsburg A (1989) Controllability, principles of naval architecture, vol 3, pp 200–258
15. ITTC (2002) ITTC recommended procedures manoeuvrability—captive model test procedure. In: Proceedings of 23rd ITTC

16. ANSYS CFX-solver theory guide, release 15 (2013)
17. Bertram V (2000) Practical ship hydrodynamics. Butterworth Publications, Oxford
18. Strom-Tejsen J (1965) A digital computer technique for the prediction of standard manoeuvres of surface ships. DTRC report 2130